

**Happy Birthday Frank!**

**(one person's view of your  
contributions to stimulating new  
research in hurricane dynamics)**

**Michael Montgomery**

**Naval Postgraduate School, Monterey USA**

**& Hurricane Research Division, NOAA/AOML**

**Miami USA**

**Collaborators: Randy Kallenbach, Wayne Schubert,  
Roger K. Smith, Sang Nguyen, John Persing, Chun-  
Chieh Wu, Yi-Hsuang**













## NOAA P3 Hurricane Research Aircraft



**Hurricane Severe Storm Sentinel (HS3)  
2 NASA Global Hawks (2012 – 2015)  
Scott Braun, PI**

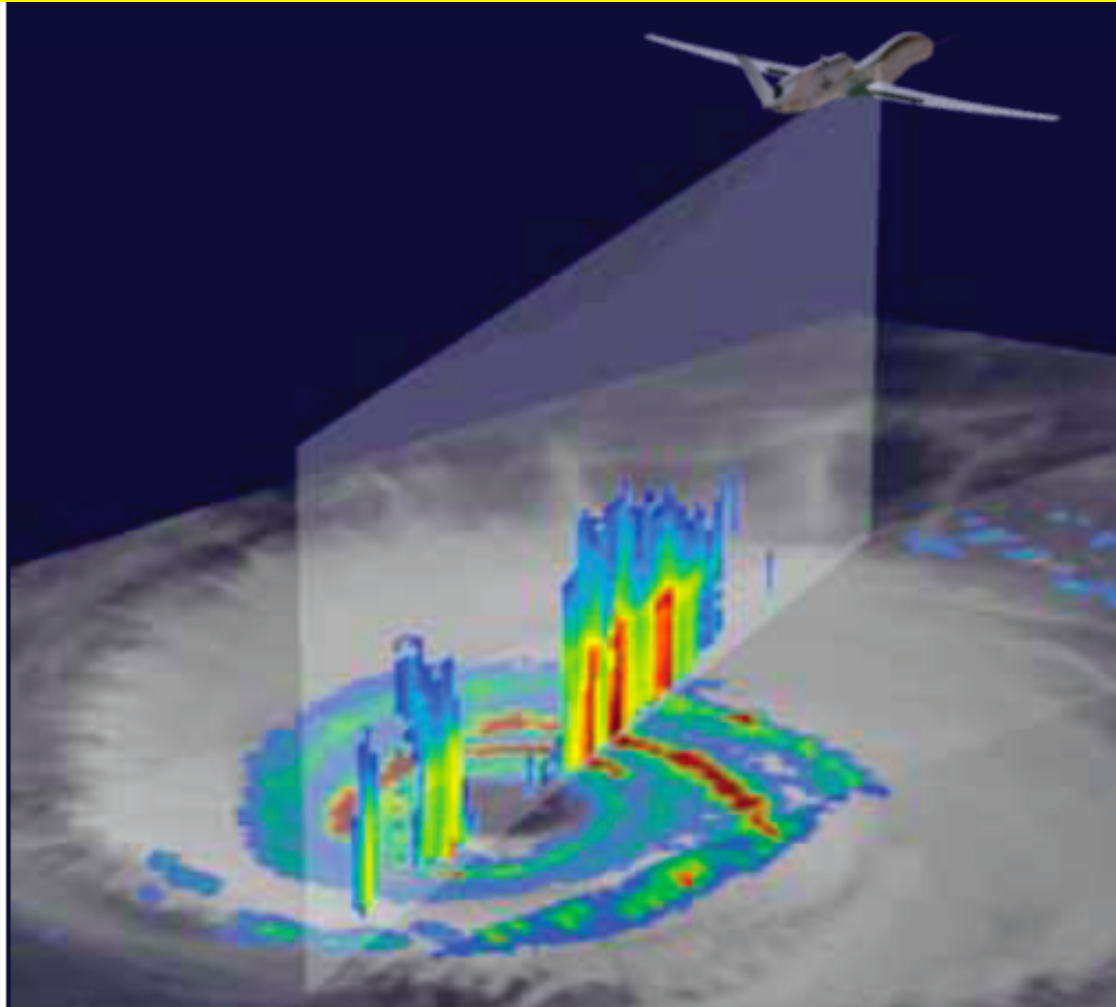
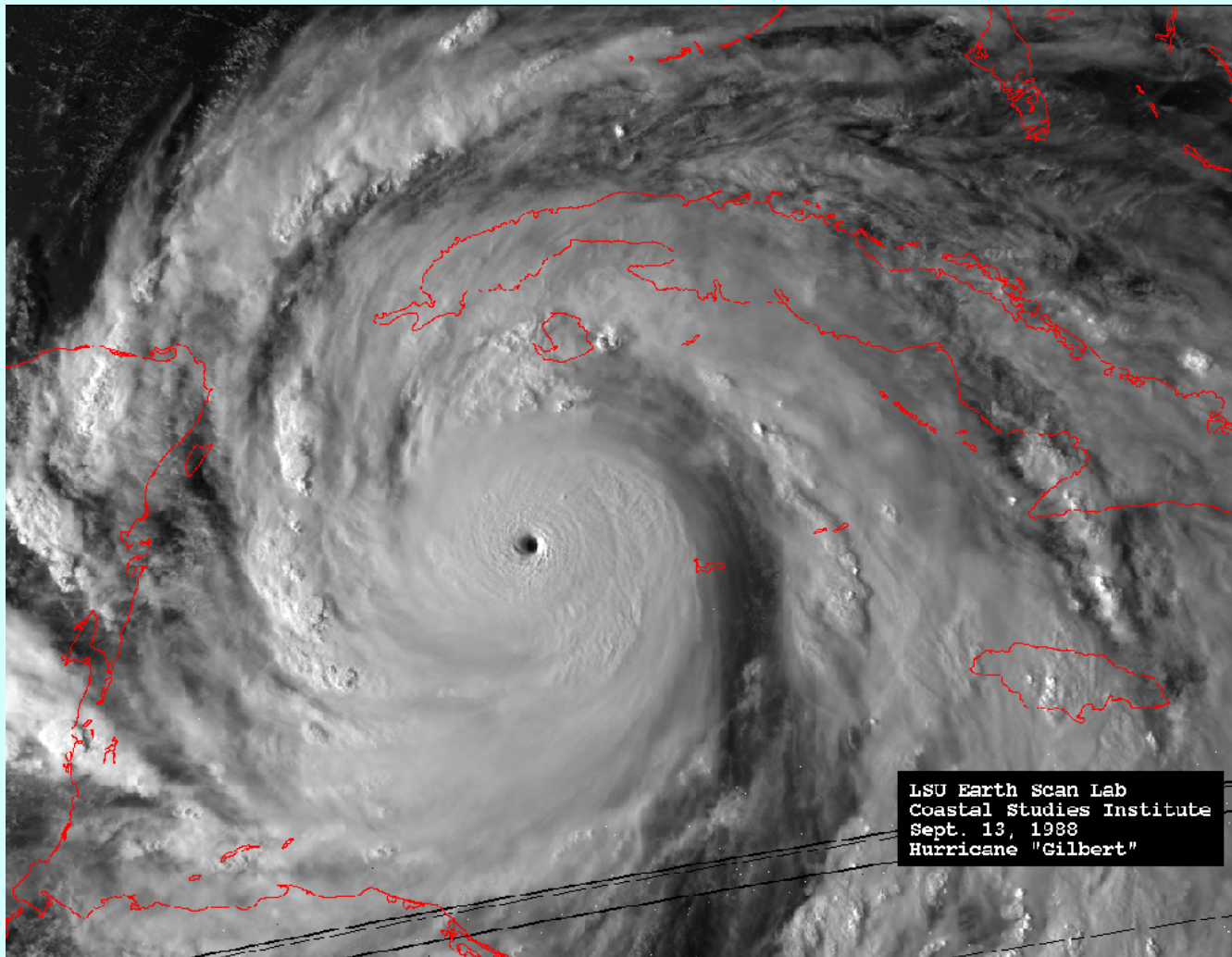


**Figure 1-1:** HS3 will collect unprecedented measurements in the storm environment and inner-core region.

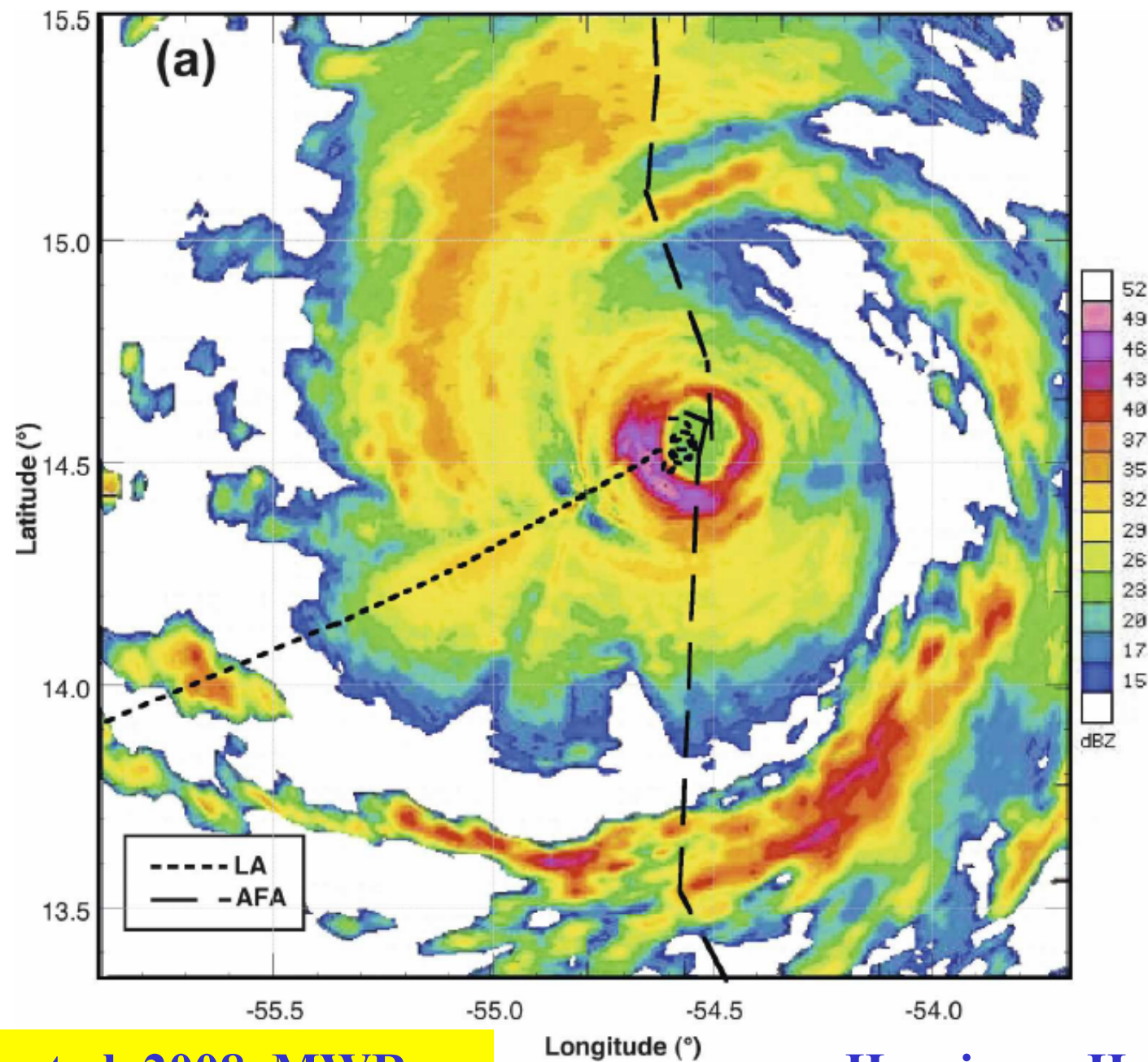






LSU Earth Scan Lab  
Coastal Studies Institute  
Sept. 13, 1988  
Hurricane "Gilbert"





Marks et al. 2008, MWR

Hurricane Hugo, 1989

## Aerial view of the eye

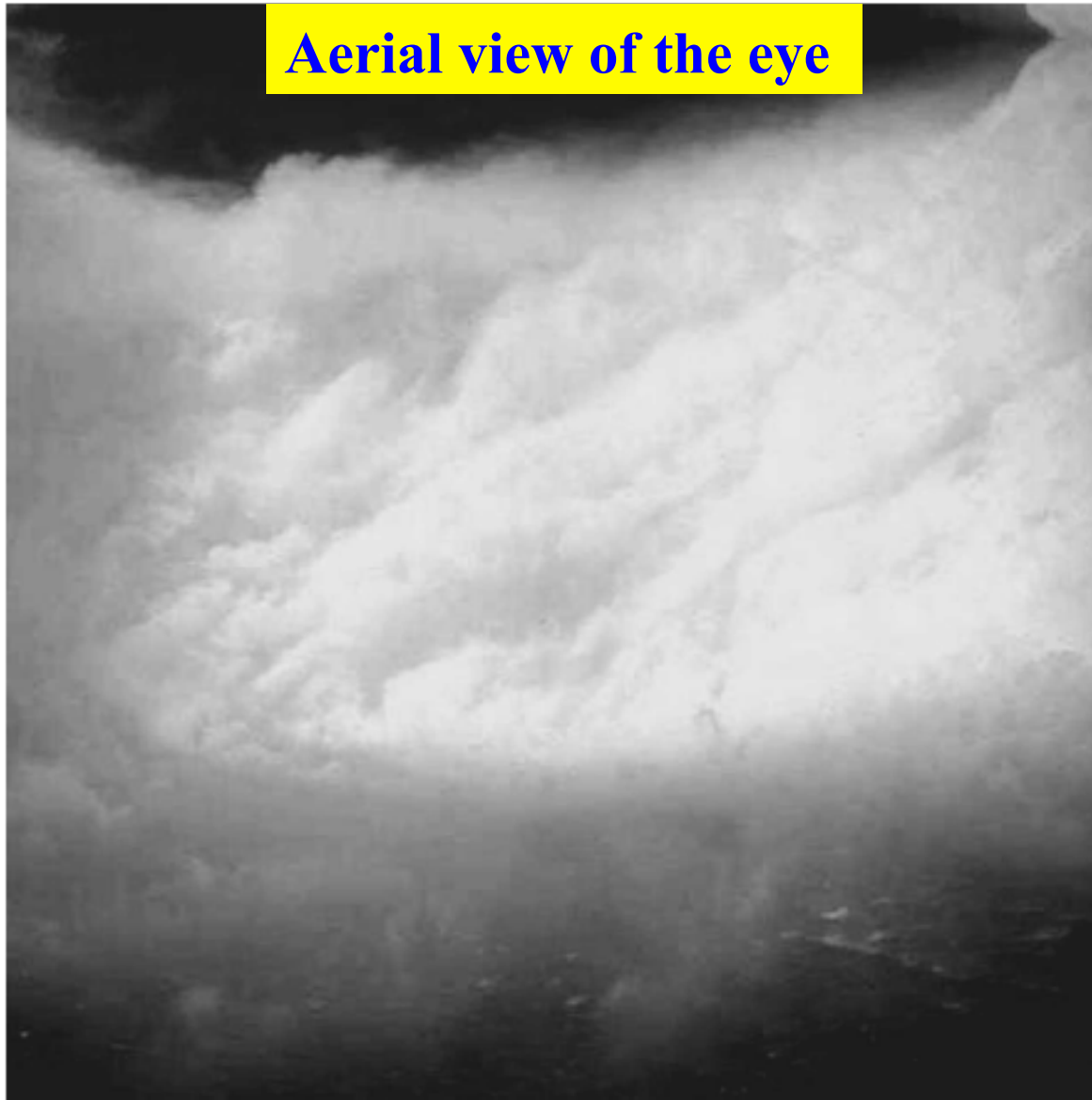


FIG. 5. Photograph of the inside of the eyewall as the aircraft circled inside the eye from 1728 to 1824 UTC showing cloud striations tilted upwind (to the right) with increasing altitude. Also visible is cirrus inside the eye at the upper edge of the eyewall.



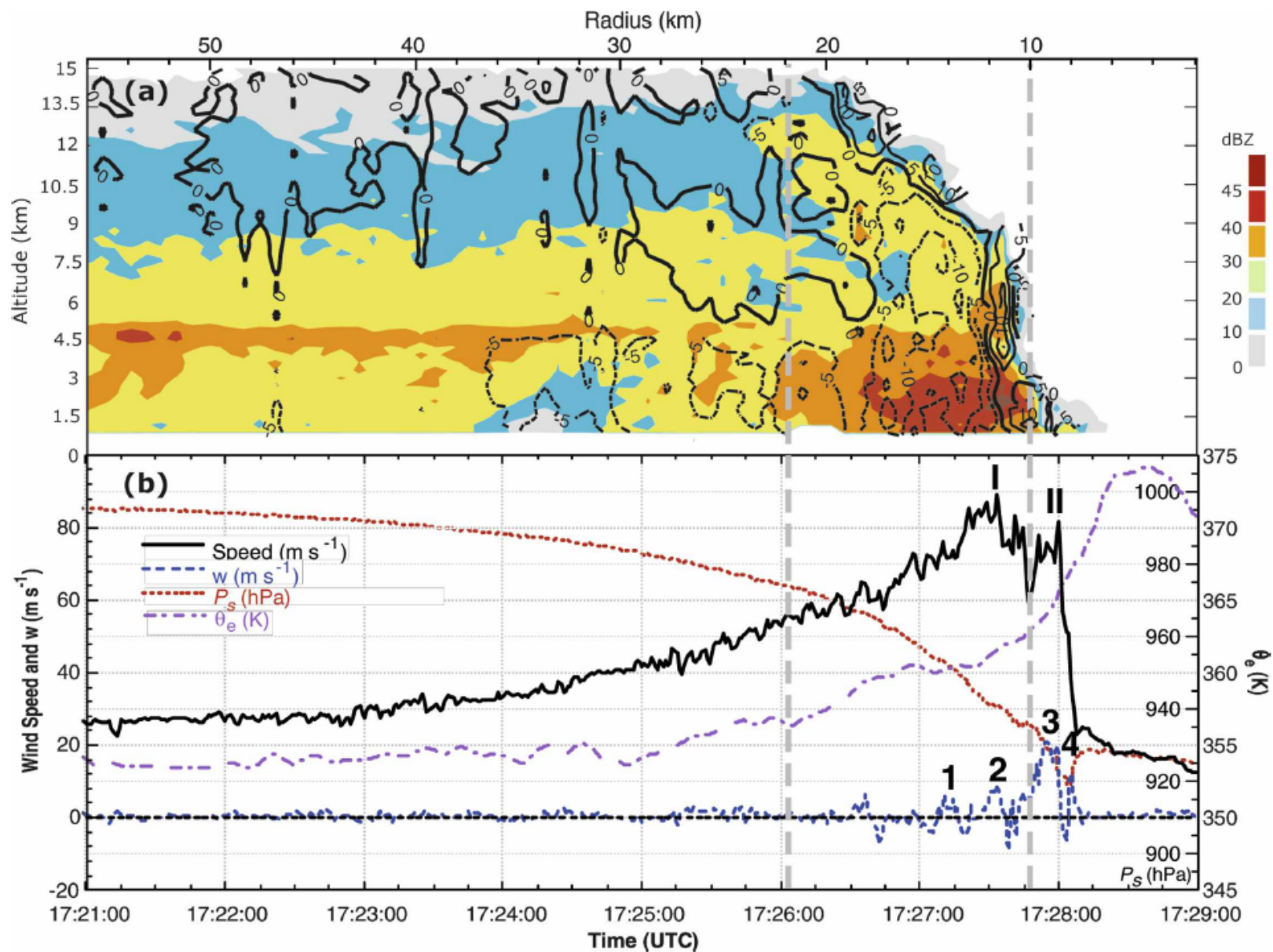


FIG. 3. (a) Time–height cross section of vertical incidence tail radar reflectivity (dBZ) from LA for 1721–1728 UTC. The LA flight track was at 450 m. Solid and dashed lines denote vertical velocity, and radar reflectivity is denoted by colors using the color scale on the right. (b) Time series plots of  $w$ , horizontal wind speed,  $P_s$ , and  $\theta_e$  for the period 1721–1730 UTC. Updrafts labeled 1, 2, 3, and 4 and wind speed peaks I and II are described in the text. The thick dashed lines in (b) approximately delineate the outer and inner radii of strong eyewall reflectivity maxima in the lower troposphere ( $1 < z < 5$ -km altitude).

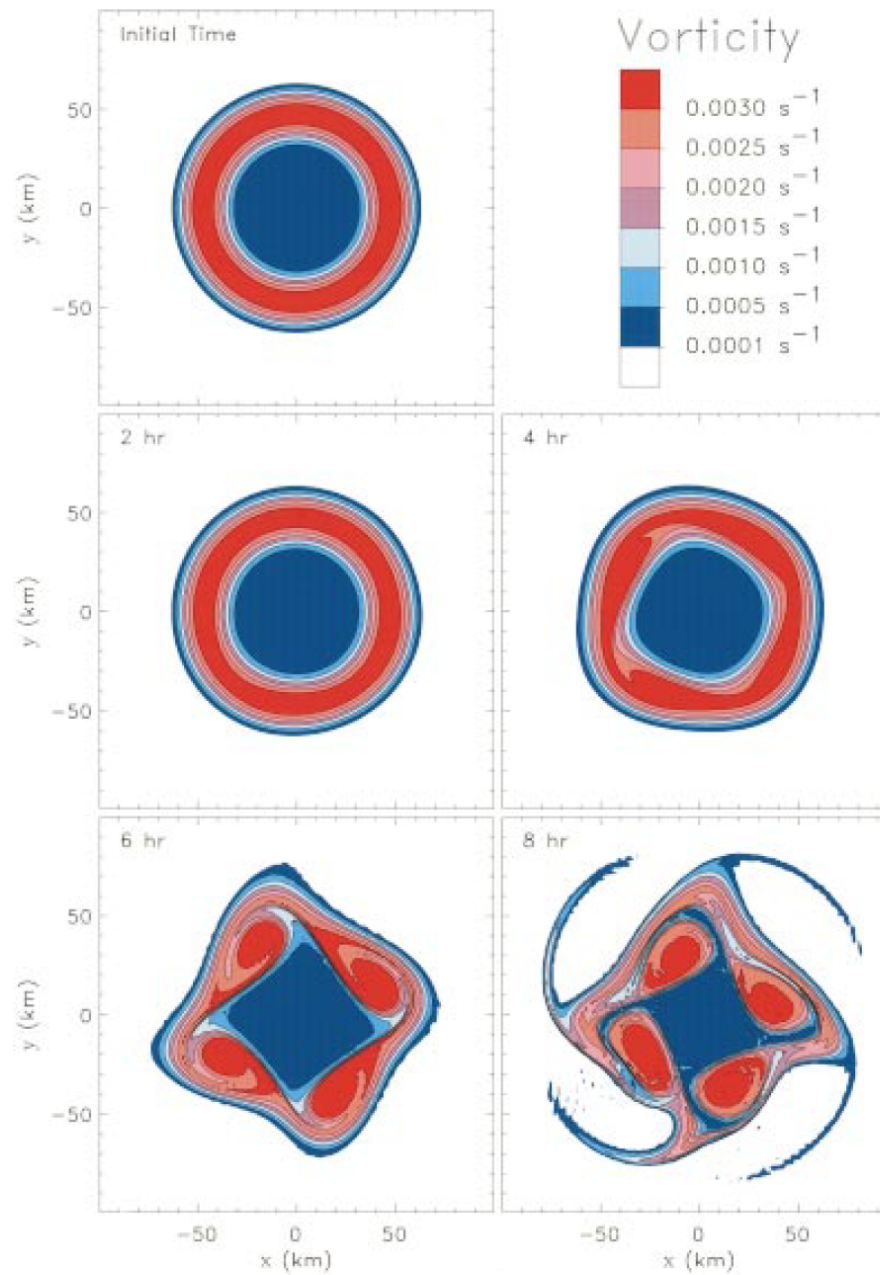
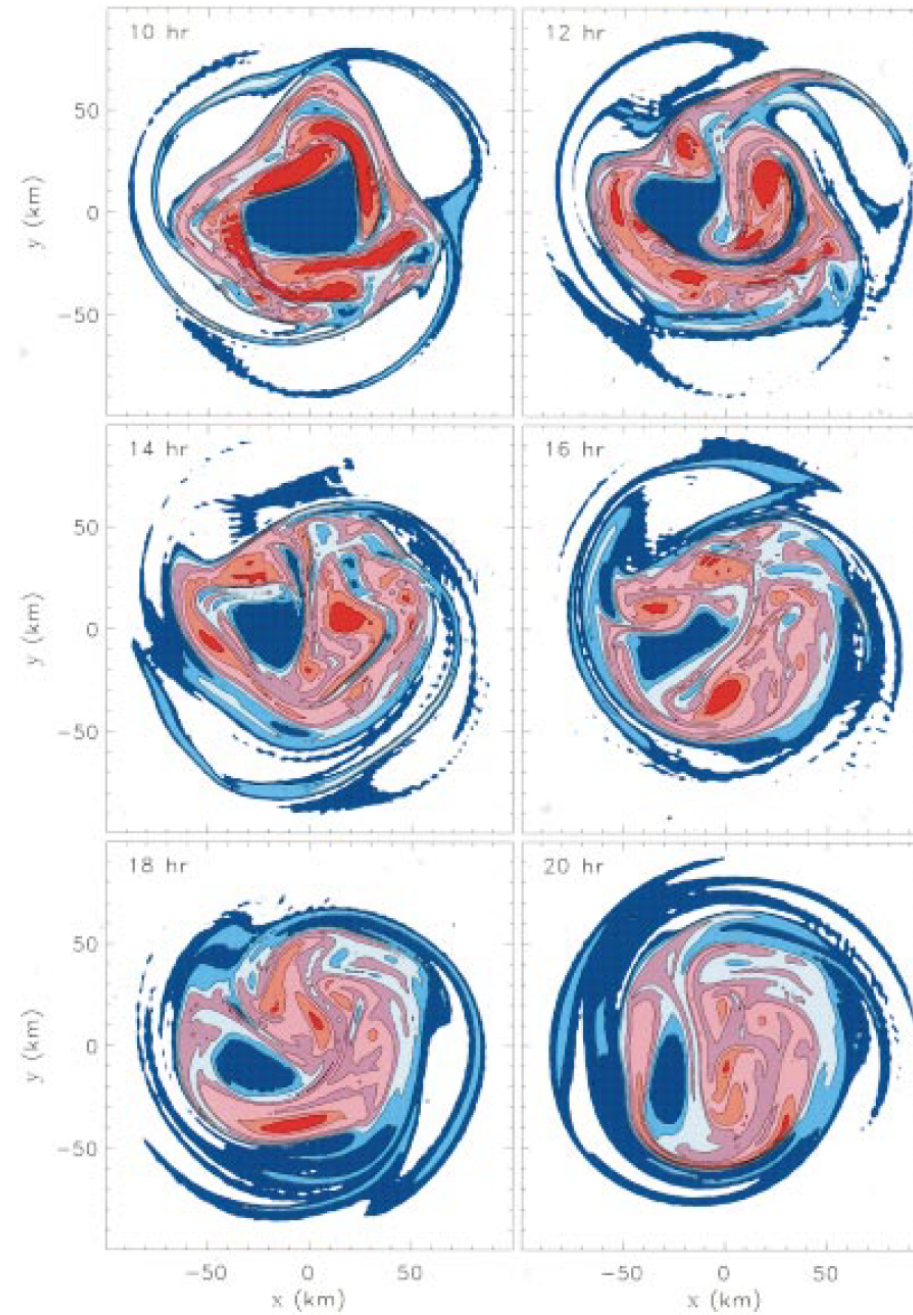


FIG. 3. Vorticity contour plots for the representative numerical experiment. The model domain is  $600 \text{ km} \times 600 \text{ km}$ , but only the inner  $200 \text{ km} \times 200 \text{ km}$  is shown. The contours begin at  $0.0005 \text{ s}^{-1}$  and are incremented by  $0.0005 \text{ s}^{-1}$ . Low vorticity values are shaded blue and high vorticity values are shaded red. (a) Vorticity from  $t = 0 \text{ h}$  to  $8 \text{ h}$ .



FIG. 3. (Continued) (b) Vorticity from  $t = 10$  h to 20 h.

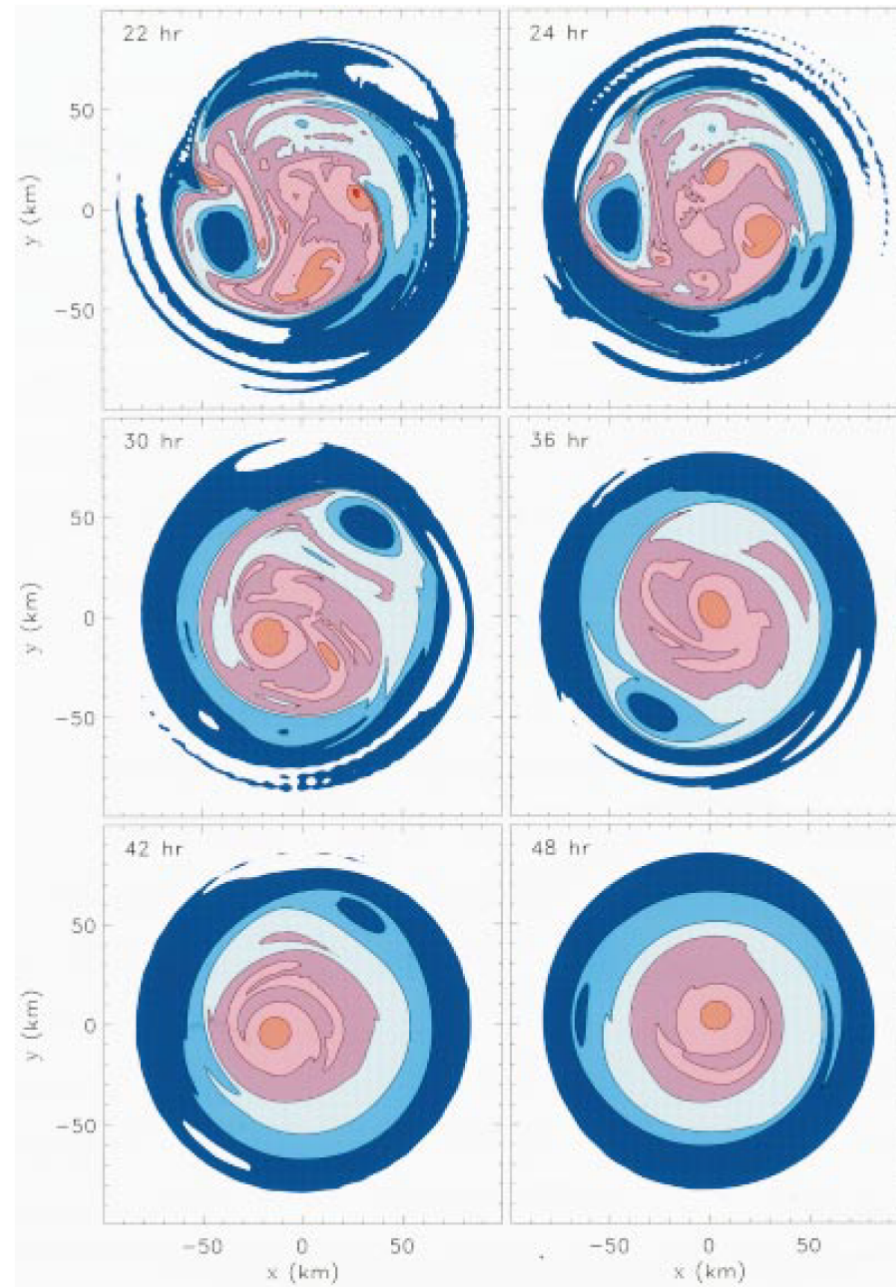


Fig. 3. (Continued) (c) Vorticity from  $t = 22$  h to 48 h with the time interval switched to 6 h after  $t = 24$  h.



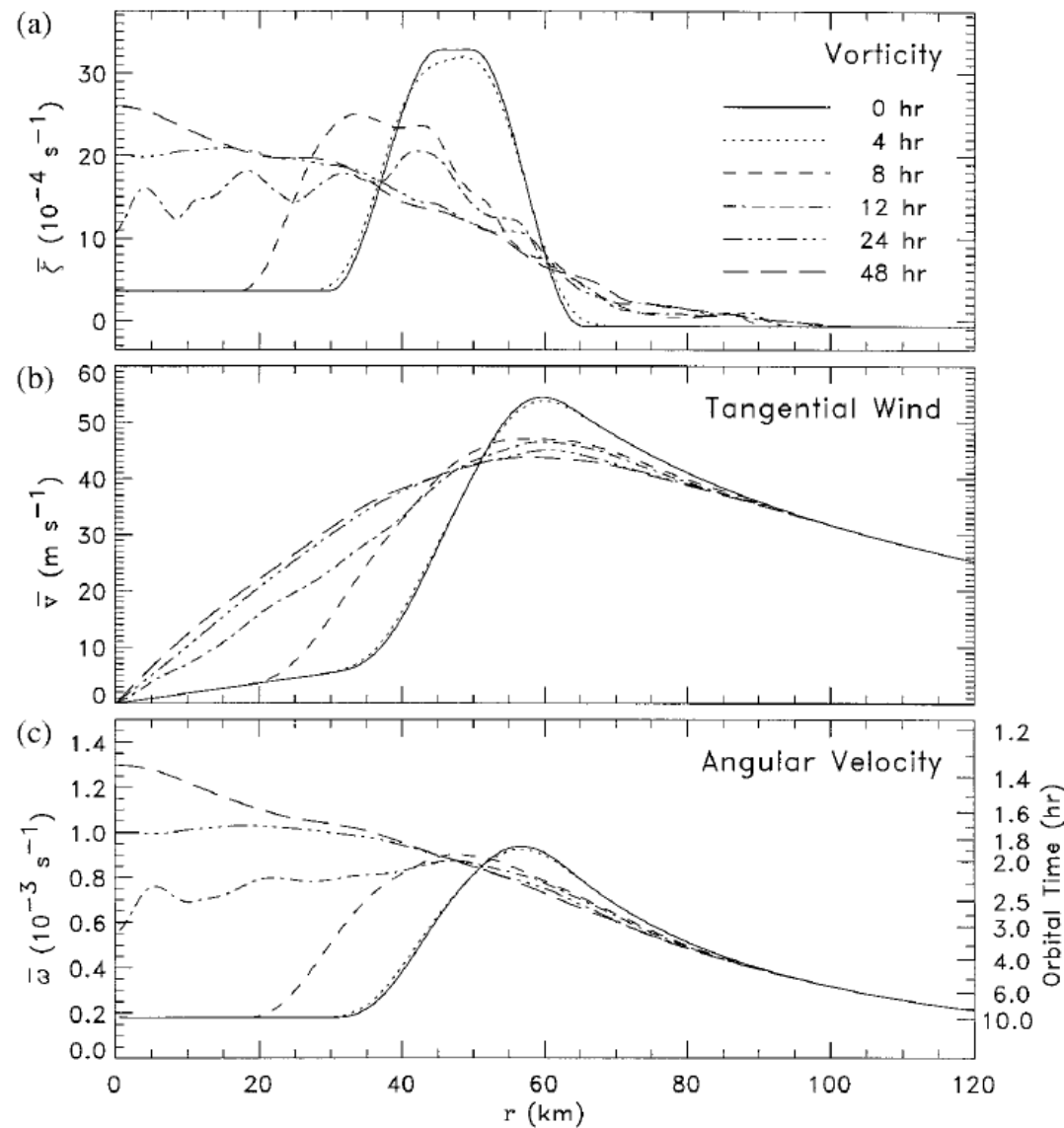


FIG. 4. Azimuthal mean vorticity ( $\bar{\zeta}$ ), tangential velocity ( $\bar{v}$ ), and angular velocity ( $\bar{\omega}$ ) for the experiment shown in Fig. 3 at the selected times  $t = 0$  (solid), 4 h (dotted), 8 h (dashed), 12 h (dash-dot), 24 h (dash-dot-dot-dot), 48 h (long dashes). The scale on the right of the bottom panel is for  $2\pi/\bar{\omega}$ , the orbital time of fluid particles (minor tick marks are for values halfway between the labeled major tick marks).

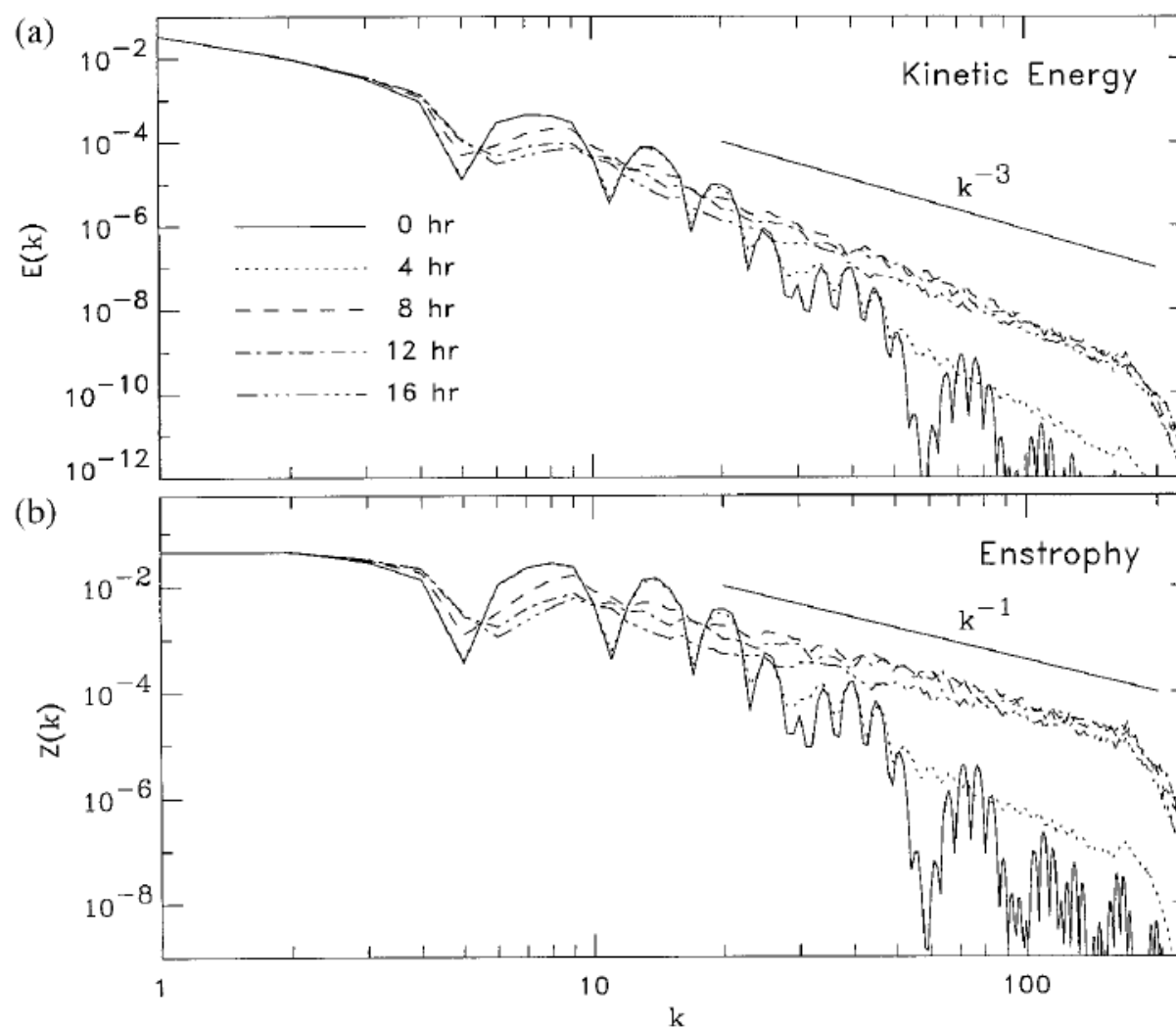


FIG. 5. Kinetic energy ( $E(k)$ ) and enstrophy ( $Z(k)$ ) spectra during the extensive mixing phase ( $0 \leq t \leq 16$  h) for the experiment shown in Fig. 3 at the selected times  $t = 0$  (solid), 4 h (dotted), 8 h (dashed), 12 h (dash-dot), and 16 h (dash-dot-dot-dot). Spectra are obtained in the usual way by binning into rings of radius  $k$  centered at the origin in Cartesian wavenumber space. The  $k^{-3}$  (energy) and  $k^{-1}$  (enstrophy) spectra, as expected for the enstrophy cascade from two-dimensional turbulence theory (neglecting logarithmic corrections), are shown for comparison.

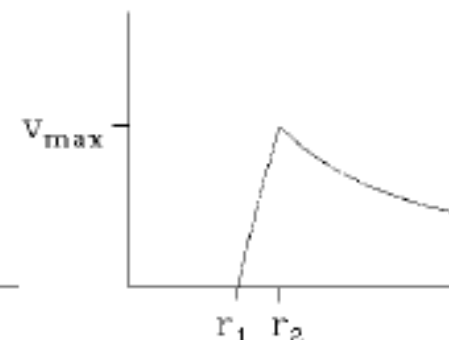
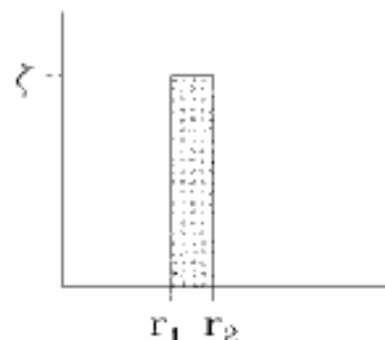
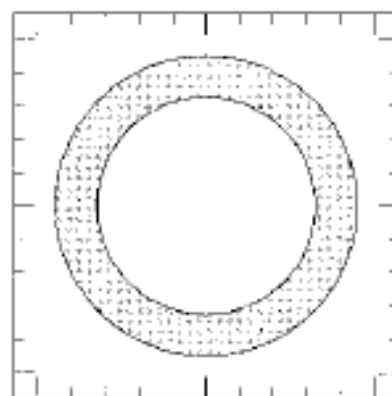


**A not so calm eye! – Ivan (2004)**



**Modis Image**

Initial Condition



End-State (without mixing)

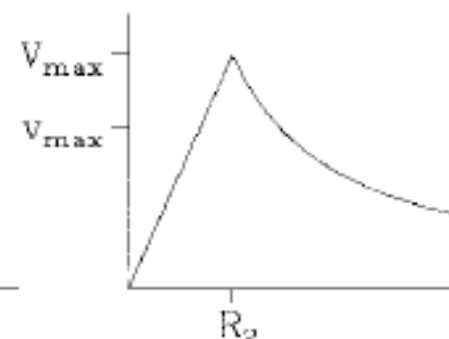
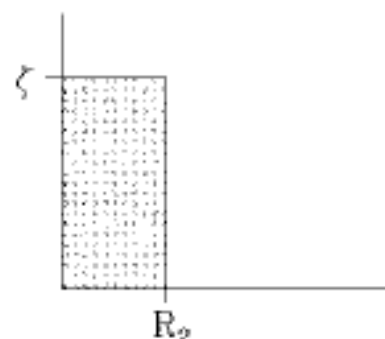
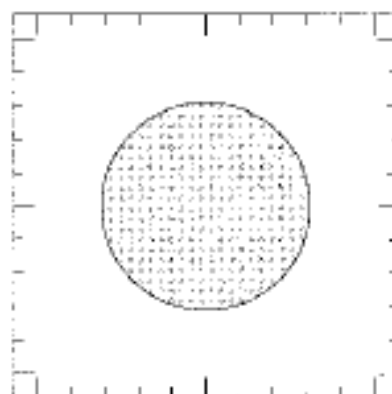


FIG. 7. Schematic of an initial vorticity distribution and the corresponding hypothesized end-state after a redistribution without mixing. The redistribution argument illustrated here is flawed because it violates kinetic energy and angular momentum invariance. This points out the necessity of vorticity mixing during the redistribution process.



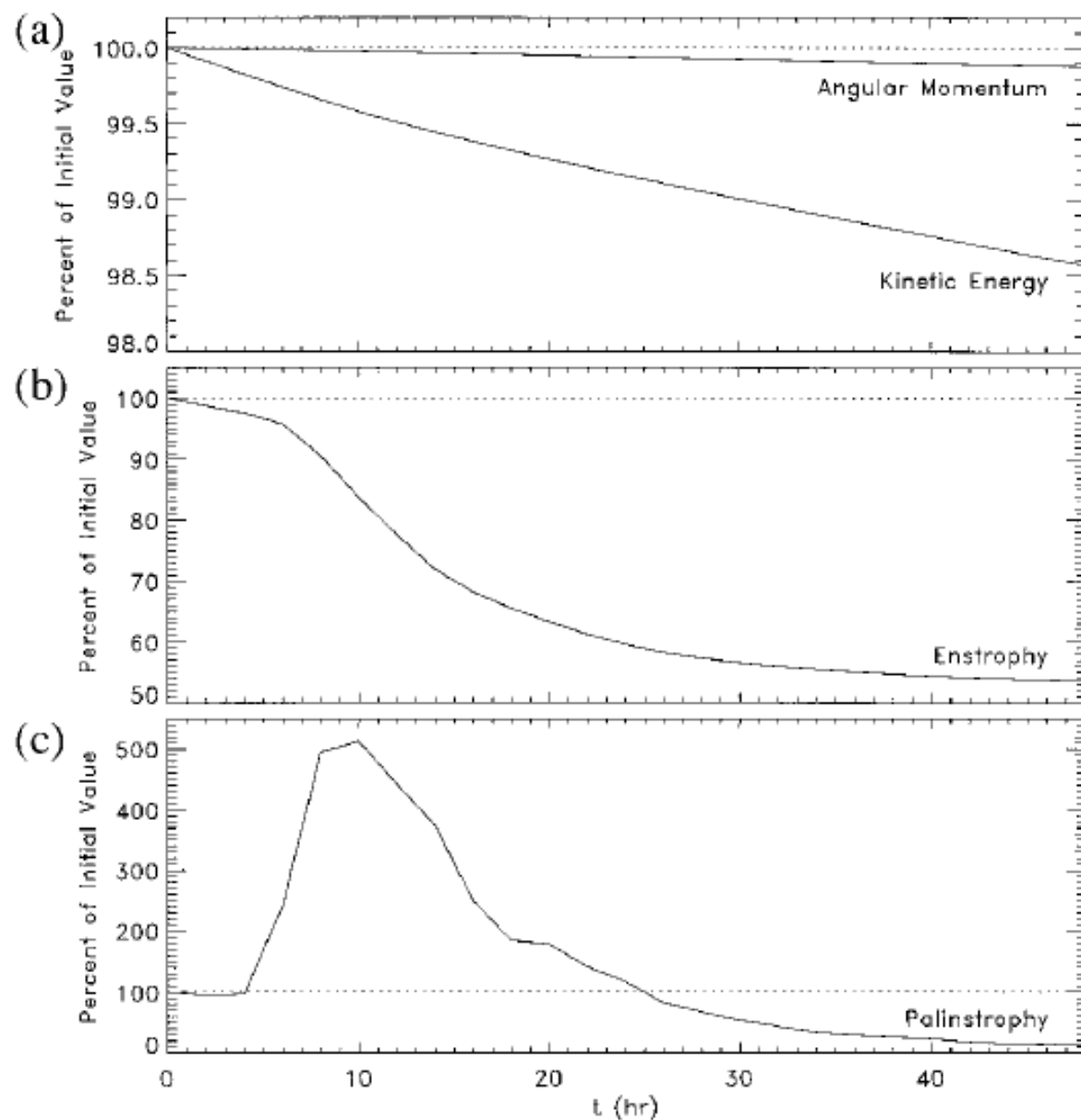


FIG. 8. Time series of kinetic energy ( $\mathcal{E}$ ), angular momentum ( $\mathcal{M}$ ), enstrophy ( $\mathcal{Z}$ ), and palinstrophy ( $\mathcal{P}$ ), all of which are integrated over the model domain for the numerical experiment shown in Fig. 3.

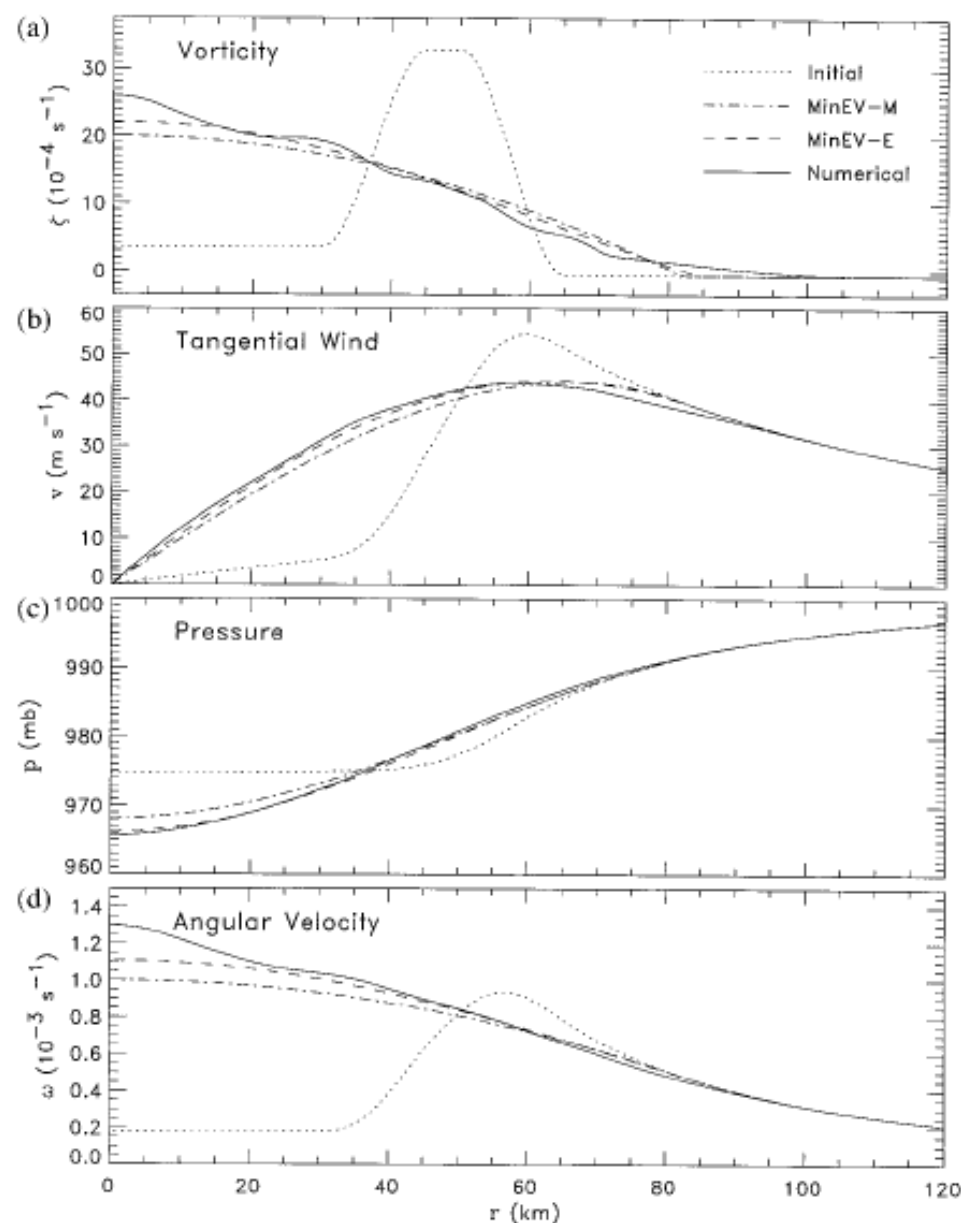


FIG. 9. Plots of the azimuthal mean vorticity  $\zeta(r)$ , tangential wind  $v(r)$ , pressure  $p(r)$ , as determined from gradient balance, and angular velocity  $\omega(r)$  for MinEV-M (dash-dotted curves), MinEV-E (dashed curves), and the direct numerical integration at 48 h (solid curves). The initial curves are shown by the dotted lines. Note that in both cases the vortex appears to be weakening in terms of tangential wind, but strengthening in terms of central pressure.

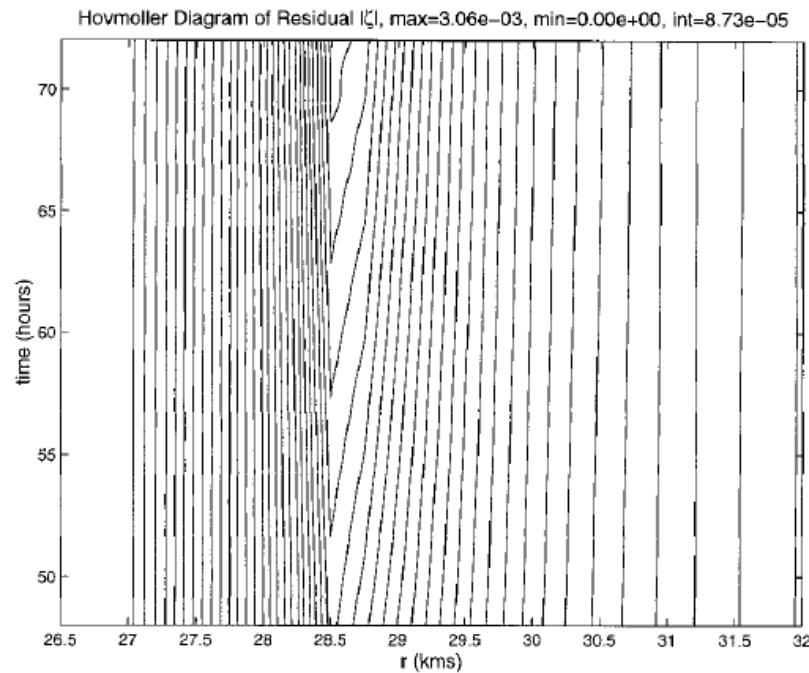


FIG. 14. Hovmöller diagram for the amplitude of the complex vorticity associated with the residual vortex-Rossby waves in the hurricane case, in the ranges  $h$  and  $km$ , showing the inward and outward propagation on either side of  $r = 28.5$  km.

*g. The effects of viscosity*

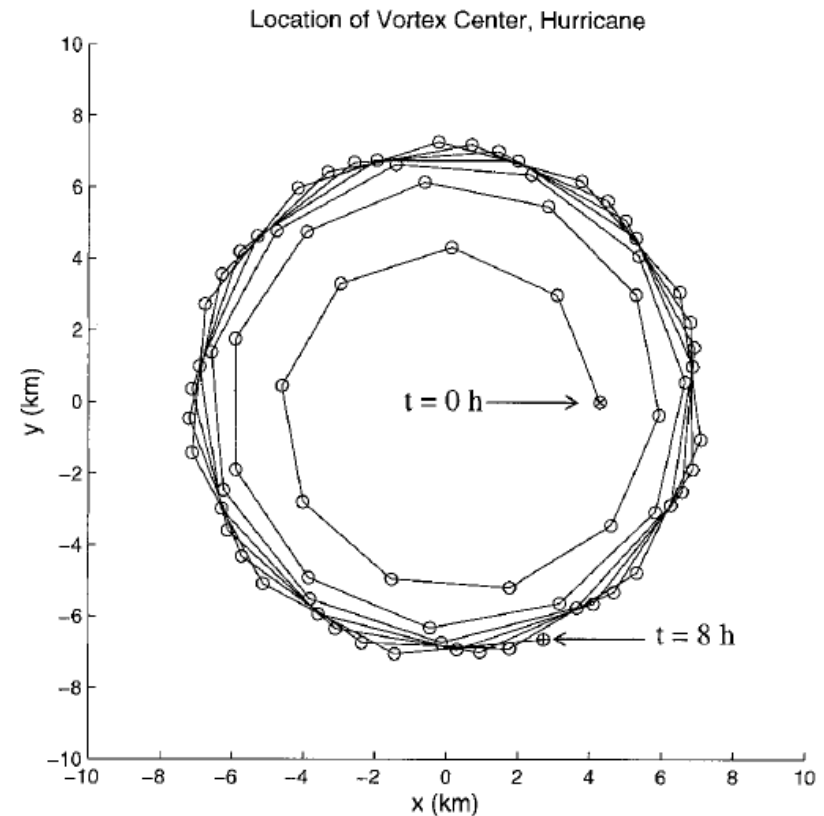


FIG. 15. Location of the vortex center in the hurricane case, marked every 400 s, for the first 8 h. Distances are in km, and the beginning and end points are indicated.



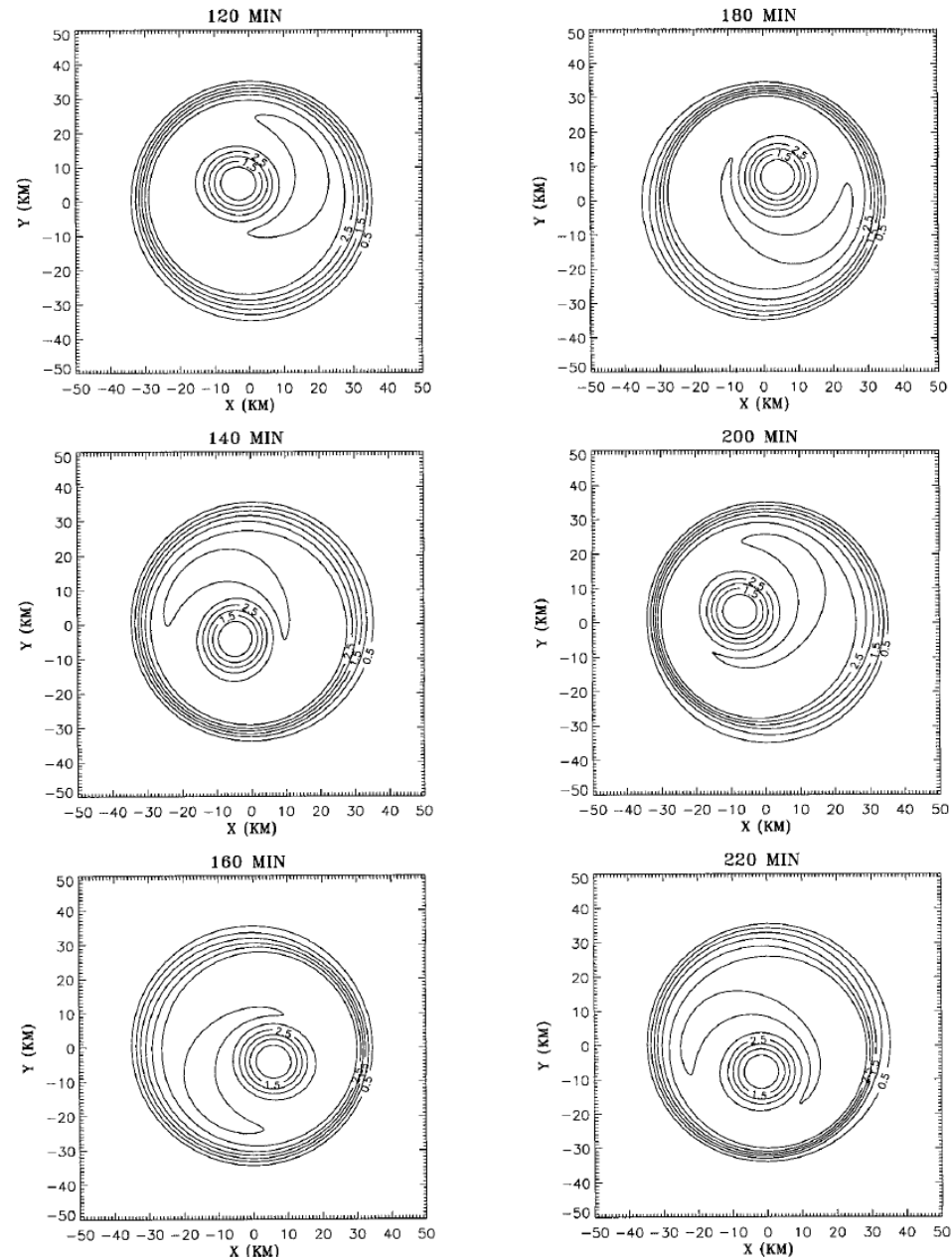
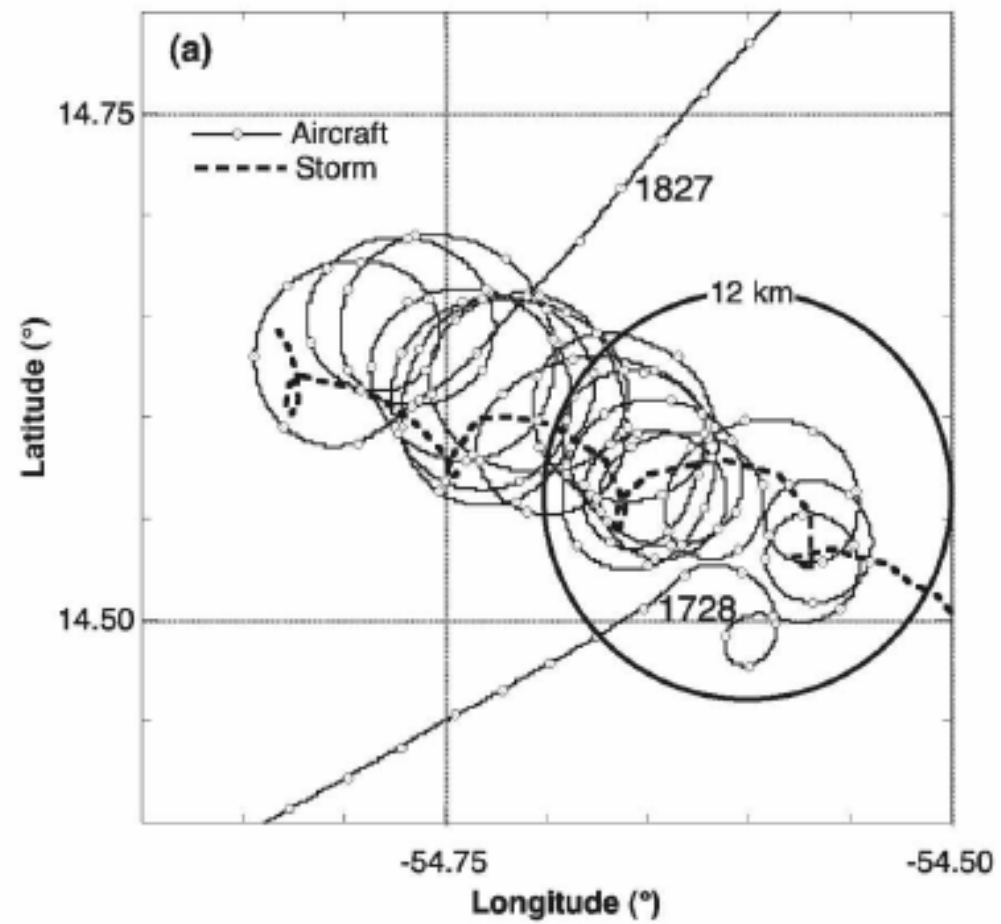


FIG. 21. Evolution of the vorticity field in the early stages of the growth of the algebraic instability in a fully nonlinear model, every 20 min from  $t = 120$  min to  $t = 220$  min. Vorticity is multiplied by  $10^3$  and the contours are labeled.

## MONTHLY WEATHER REVIEW



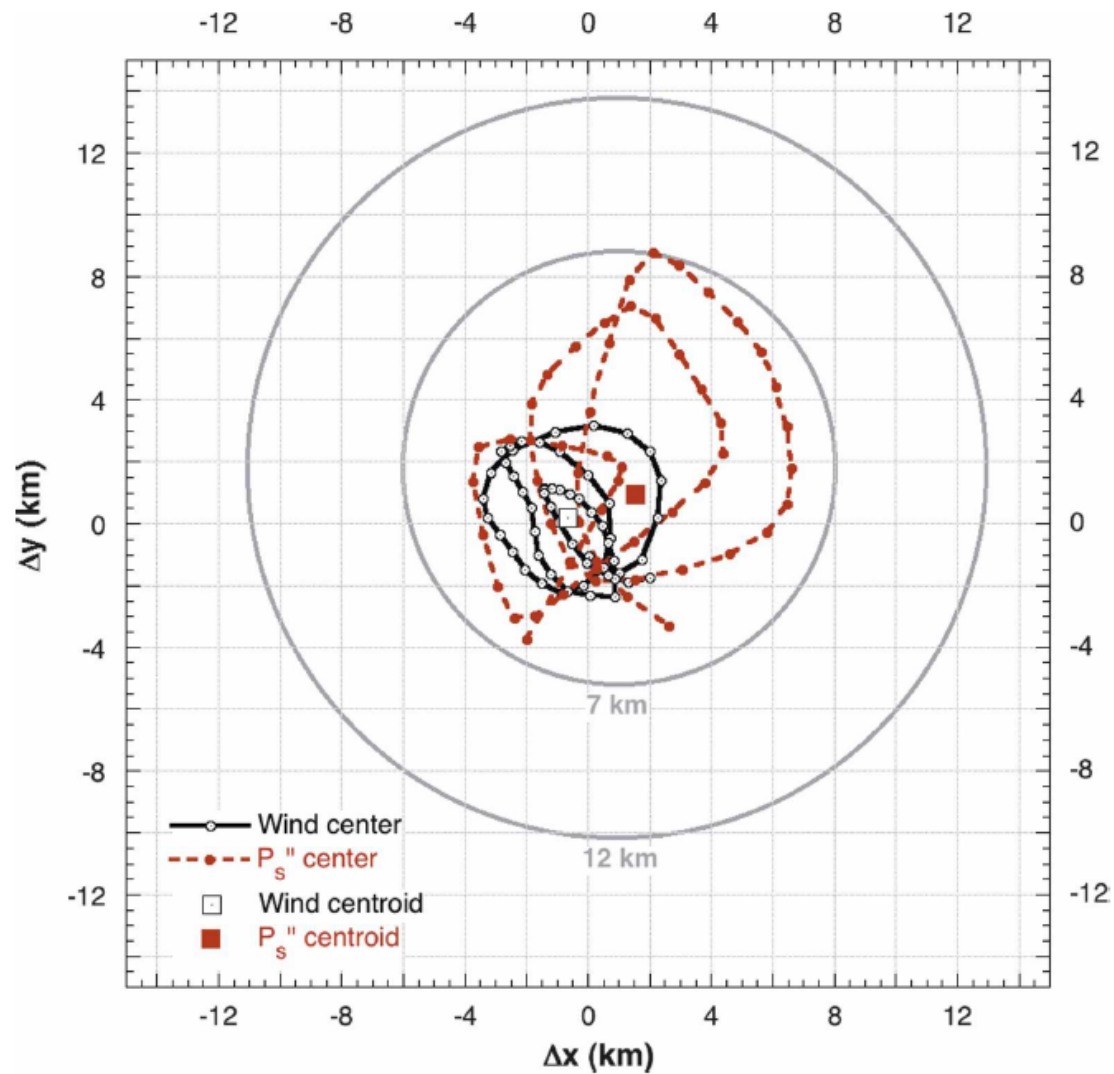


FIG. 9. East-west ( $\Delta x$ ) and north-south ( $\Delta y$ ) deviations of storm-relative wind (open circles) and  $P_s''$  centers (solid circles) from the linear least squares fit of the wind centers from 1728 to 1824 UTC. The wind center centroid is denoted by the white square and that for the  $P_s''$  centers by the red square. The 7- and 12-km circles are centered on the centroid of the pressure centers to denote the radii of the radar eye and reflectivity maximum, respectively. Storm motion was removed.



### *b. Eyewall-scale trochoidal mode*

Earlier analyses using the data obtained during LA's orbits within the eye originally led the first two authors to hypothesize that the EVM was long-lived, making three orbits around the eye in 1 h (Marks and Black 1990; Black and Marks 1991). Since then, however, an alternative hypothesis was developed here in which the observed evolution of the circulation within the eye is a trochoidal oscillation or wobble of the eye that is expected to stimulate and/or accompany the vorticity-mixing process described above. Evidence supporting this hypothesis and its relation to recent theoretical predictions is summarized here.

Following the encounter with the EVM, the aircraft repeatedly penetrated local wind and pressure minima as it orbited within the eye and climbed to a safer altitude. From Fig. 8 it is evident that both the wind and pressure centers exhibited a trochoidal-like oscillation, making three orbits while undergoing a mean translation speed of  $9 \text{ m s}^{-1}$ . The pressure centers lagged the wind centers slightly in time, with a larger orbital radius ( $\sim 6.5 \text{ km}$ ) than that for the wind center ( $\sim 2 \text{ km}$ ). After removing the storm motion, the relative wind and pressure centers are found to orbit around a common locus (see Fig. 9) with a rotation period of approximately 19 min. The longevity ( $>1 \text{ h}$ ) and 19-min rotation period of the wind and pressure centers strongly suggest a persistent wobble of the storm circulation center.

## Structure of the Eye and Eyewall of Hurricane Hugo (1989)

FRANK D. MARKS AND PETER G. BLACK

*Hurricane Research Division, NOAA/AOML, Miami, Florida*

MICHAEL T. MONTGOMERY

*Naval Postgraduate School, Monterey, California*

ROBERT W. BURPEE\*

*Cooperative Institute for Marine and Atmospheric Studies, University of Miami, Miami, Florida*

(Manuscript received 31 October 2006, in final form 12 April 2007)

### ABSTRACT

On 15 September 1989, one of NOAA's WP-3D research aircraft, N42RF [lower aircraft (LA)], penetrated the eyewall of Hurricane Hugo. The aircraft had an engine fail in severe turbulence while passing the radius of maximum wind and before entering the eye at 450-m altitude. After the aircraft returned to controlled flight within the 7-km radius eye, it gained altitude gradually as it orbited in the eye. Observations taken during this period provide an updated model of the inner-core structure of an intense hurricane and suggest that LA penetrated an intense cyclonic vorticity maximum adjacent to the strongest convection in the eyewall [eyewall vorticity maximum (EVM)]. This EVM was distinct from the vortex-scale cyclonic circulation observed to orbit within the eye three times during the 1 h that LA circled in the eye. At the time, Hugo had been deepening rapidly for 12 h. The maximum flight-level tangential wind was  $89 \text{ m s}^{-1}$  at a radius of 12.5 km; however, the primary vortex peak tangential wind, derived from a 100-s filter of the flight-level data, was estimated to be  $70 \text{ m s}^{-1}$ , also at 12.5-km radius. The primary vortex tangential wind was in approximate gradient wind balance, was characterized by a peak in angular velocity just inside the radius of maximum wind, and had an annular vorticity structure slightly interior to the angular velocity maximum. The EVM along the aircraft's track was roughly 1 km in diameter with a peak cyclonic vorticity of  $1.25 \times 10^{-1} \text{ s}^{-1}$ . The larger circulation center, with a diameter  $>15 \text{ km}$ , was observed within the eye and exhibited an average orbital period of 19 min. This period is about the same as that of the angular velocity maximum of the axisymmetric mean vortex and is in reasonable agreement with recent theoretical and model predictions of a persistent trochoidal "wobble" of circulation centers in mature hurricane-like vortices. This study is the first with in situ documentation of these vortical entities, which were recently hypothesized to be elements of a lower-tropospheric eye/eyewall mixing mechanism that supports strong storms.







---

## Paradigms for tropical-cyclone intensification

Michael T. Montgomery<sup>a</sup> \* and Roger K. Smith<sup>b</sup>

<sup>b</sup> *Meteorological Institute, University of Munich, Munich, Germany*

<sup>a</sup> *Dept. of Meteorology, Naval Postgraduate School, Monterey, CA & NOAA's Hurricane Research Division, Miami, FL, USA.*

---

**Abstract:** We review four paradigms of tropical-cyclone intensification, focusing on a new paradigm articulated in a series of recent papers by ourselves and colleagues. The new paradigm views the intensification process as intrinsically asymmetric and dominated by deep convective vortex structures. These convective structures, or “vortical hot towers”, exhibit a degree of randomness that has implications for the predictability of asymmetric features of the developing storm on the convective scale. The vortical hot towers possess local buoyancy relative to the azimuthally-averaged virtual temperature field of the warm-cored vortex. Using an idealized, three-dimensional, non-hydrostatic numerical model, we have shown that, from an axisymmetric viewpoint, the spin-up of the inner core is associated with the convergence of absolute angular momentum in the boundary layer, where this quantity is not conserved. While surface moisture fluxes are required for storm intensification, the intensification does not require the ‘evaporation-wind’ feedback process that forms the basis of an earlier paradigm. The details of the intensification process as well as the structure of the mature cyclone are found to be sensitive to the boundary layer parameterization used in the model, although they are less sensitive to the surface exchange coefficients, contrary to the previous results obtained from axisymmetric balanced models. Balanced and unbalanced contributions to the intensification process are highlighted also. Copyright © 2009 Royal Meteorological Society



**Thank you Frank and  
Happy Birthday!**